Near-GeV acceleration of electrons by a self-guided laser pulse

Contact s.nagel@imperial.ac.uk

S. Kneip, S. R. Nagel, S. P. D. Mangles, C. Bellei, A. E. Dangor, C. Palmer, J. Schreiber and Z. Najmudin
The Blackett Laboratory, Imperial College London, SW7 2BZ, UK

S. Martins, F. Fiuza, R. Fonseca, J. Vieira and L. O. Silva
GoLP/Inst Plasmas & Fusao Nucl, Instituto Superior Tecnico, Lisbon, Portugal

O. Chekhlov, R. J. Clarke, E. J. Divall, K. G. Ertel, P. S. Foster, S. J. Hawkes, R. Heathcote, C. J. Hooker, P. P. Rajeev and M. J. V. Streeter
Central Laser Facility, STFC, Rutherford Appleton Laboratory, HSIC, Didcot, Oxon OX11 0QX, UK

K. Krushelnick and K. Ta Phuoc
Center for Ultrafast Optical Science, University of Michigan, Ann Arbor 48109 USA

W. B. Mori
Department of Physics and Astronomy and Department of Electrical Engineering, UCLA, Los Angeles, California 90095, USA

Recent advances in plasma based particle acceleration have demonstrated energy gains in excess of gigaelectronvolts. In an accelerator driven by the 42 GeV electron beam at the Stanford Linear Accelerator (SLAC), a doubling of the energy of properly phased electrons was demonstrated in a distance of only 30 cm[1]. Plasma accelerators driven by high intensity lasers have also demonstrated gain up to 1 GeV in 3.3 cm[2]. Such accelerators would have profound implications for high energy physics and producing novel radiation sources. For laser driven plasma accelerators, it has been thought that to obtain this energy gain, an exter nal guiding structure is required to maintain high laser intensity over the acceleration length. Using Astra Gemini, the first of a new generation of multi-100 TW class laser facilities, we demonstrate, that this is not the case and that GeV level acceleration can be achieved without an external guide. Fully relativistic three-dimensional simulations confirm that intensity amplification of the self-guided laser pulse generates a plasma wave of sufficient amplitude to allow GeV level electron energy gain in a distance of 1 cm. The studies presented here provide evidence for the scalability of self-guided laser wakefield accelerators from 0.1 to 1 GeV and beyond.

Plasma-based accelerators can support electric fields several orders of magnitude greater than conventional accelerators, and as a result, can be substantially more compact. In the laser wakefield scheme[3], the accelerating field is generated by the ponderomotive force of an intense laser pulse, which pushes electrons away from regions of higher laser intensity. The electrons return due to the force generated by their separation from the stationary background plasma ions. The electrons overshoot their equilibrium position and begin to oscillate in the wake of the intense laser field. Since it travels with the laser pulse, the wakefield has a phase velocity close to the speed of light. Charged particles travelling at relativistic speeds in the accelerating phase of the mainly electrostatic oscillation can become trapped and gain energy.

Trapping particles within the micron sized accelerating structure is not trivial. However, a wakefield driven to a sufficiently large amplitude, can trap and accelerate electrons from the plasma itself, due to wavebreaking[4,5]. Recently it has been shown that this self-injection can be sufficiently localised within the multi-dimensional accelerating structure, such that all the injected electrons are accelerated to almost the same energy, leading to beams with comparatively low energy spread[6-8].

The wakefield travels at close to but less than the speed of light c; for densities less than the critical density ($n_e \ll n_c$), the relativistic factor associated with the wave is $\gamma_{ph} \simeq (\omega_0/\omega_p)$. As the electrons are accelerated, they rapidly reach speeds very close to c, and eventually out-run the wave. Hence the electrons cease to be accelerated after a dephasing length, $Ld \approx \gamma_{ph}^2 \lambda_p$, where $\lambda_p = 2\pi c/\omega_p$ is the plasma wave wavelength. For a three-dimensional non-linear wake in the blow-out regime, the maximum energy gain due to dephasing, is $W_{max} \approx \frac{2}{3} a_0 (n_c/n_e)$[9], where a_0 is a measure of the laser intensity $a_0 \propto \sqrt{I}$. Hence energy gain *increases* with decreasing plasma density, mainly because the dephasing length ($\propto n_e^{-3/2}$) also increases.

The dephasing length is typically longer than the length over which the laser defocuses in vacuum, the Rayleigh length ~ z_R. For an ideal gaussian pulse $z_R \approx \pi w_0^2/\lambda_0$, for laser wavelength λ_0. For a laser focused to a spot diameter of $2w_0 \approx \lambda_p$, which is close to ideal for the blow-out regime[9,10], then $z_R \propto n_e^{-1}$. Hence by going to lower density, to obtain higher final energy, the ratio $L_d/z_R \approx \omega_0/\pi\omega_p = \gamma_{ph}/\pi$ increases. So, even if a laser pulse is intense enough to inject electrons into a wakefield, there is no guarantee that it can accelerate them sufficiently far to achieve maximum energy gain.

Therefore, some form of optical guiding is required to ensure acceleration over a dephasing length. It has been commonly thought that self-guiding for the short pulses required for LWFA is not possible due to a

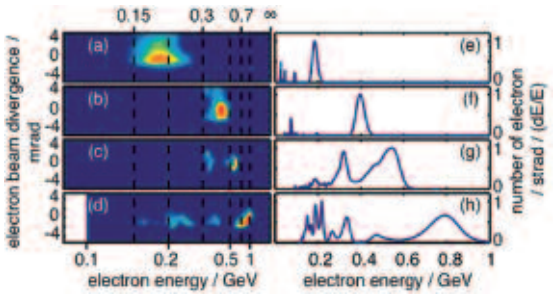

Figure 1. 2D raw images and 1D lineouts of the electron spectra. Spectrally dispersed electron beam shown at the exit of the magnetic spectrometer for gas jet lengths (a) 3 mm, (b) 5 mm (c) 8 mm and (d) 10 mm, at a plasma density of n_e = 5.7 (±0.2) × 10^{18} cm^{-3} with 10 J of laser energy on target in a τ = 55 fs pulse. The spectra exhibit mono and poly-energetic electron beams. Averaging several hundred shots with plasma densities 2 – 12 × 10^{18} cm^{-3}, the root mean square beam position was stable to < 5 mrad. For the highest energy beams, the pointing variation was < 4 mrad, and the 1/*e* divergence was 3.6 mrad in the direction of laser polarisation and 3 mrad in the or thogonal direction. This asymmetr y can be attributed to an interaction between laser and electrons in the plasma bubble[23], which increases at higher plasma densities. An increase of beam divergence was also obser ved at lower than optimum densities and was the result of less than ideal guiding at the very low densities. (e) to (h) represent lineouts of (a) to (d), that have been deconvolved to give the electron number per solid angle and relative energy spread *dE*/*E*, normalised to unity.

cancellation of relativistic and ponderomotive terms[11]. Therefore, the use of plasma waveguides has been extensively explored[2,12,13]. However, experiments without plasma channels have also demonstrated acceleration close to the dephasing length[8,10]. In these experiments the plasma density was relatively high ($n_e \geq 10^{19} cm^{-3}$) so the acceleration length was on the order of millimeters and $a_0 \approx 1$, leading to energy gains ~ 0.1 GeV and a complicated laser evolution and injection process. Even for these short dephasing distances (L_d ~ 0.1mm) self-guiding was required. Despite the cancellation of effects at the front of the laser, sufficient self-guiding of short pulses indeed occurs due to a combination of relativistic mass modifications to the refractive index and ponderomotive blowout that occurs when $P/Pc > 1$ and $a_0 \geq 2$ where $P_c = 17(n_c/n_e)$ GW. For sufficiently large a_0 a nearly spherical wake structure is formed[14] which is often referred to as a plasma bubble[15]. For properly matched beams this bubble can trap the bulk of the laser while the leading edge diffracts slowly as it pump depletes into the wake[9,10,15].

For acceleration to higher energies with a self-guided pulse, we must employ lower densities to extend the dephasing length. Not only does this increase the power requirement for self-focusing ($P_c \propto n_e^{-1}$), but also the laser power required to obtain a threshold a_0 for injection, since the bubble size also increases with decreasing density.

In this letter we report on the first experiments performed with self-guided laser driven plasma accelerators using greater than 200 TW laser pulses. We show that at these high powers, self-guiding in the nonlinear wakefield regime can extend the interaction to a distance exceeding the dephasing length even without an external guiding channel (> 1 cm ~ $10z_R$). We also show that, as a result, the maximum observed electron energy rises with increasing acceleration length, up to a maximum of ≈ 0.8 GeV. These high energies are a result of intensity (a_0) amplification of the laser pulse self-guided over such long distances, and is the first identification of acceleration by highly non-linear plasma waves.

In the experiments, an intense short pulse laser (τ ≃ 55 fs, $a_0 \simeq 3.9$) was focused onto the front edge of a helium plasma of varying length (see methods section). The resulting electron spectra obtained at a fixed density of $n_e = 5.7(\pm 0.2) \times 10^{18}$ cm^{-3} are shown in figure 1. High-energy electron beams of narrow energy spread are produced, whose peak energy W_{max} increases with increasing length. This increase of energy with length shown in figure 2 inset implies two things. First it suggests that electrons are self-injected early in the interaction. It is thought that $a_0 \gtrsim 4.2$ must be approximately larger than 4.2 for self-injection[12], which compares to our initial $a_0 = 3.9$. Hence less self-evolution is necessary to raise the laser intensity to that required for injection here as compared to previous self-injection experiments, which were performed with $a_0 \sim 1$[6-8]. The reduced evolution phase before injection is also supported by observation of an electron beam on every shot at the optimum conditions. Secondly the rate of energy gain with plasma length implies a lower acceleration than in previous experiments at both higher[16] and comparable densities[17]. As described below this is an indication of complex dynamics within the non-linear wake, rather than less acceleration. In fact, the electric field actually increases due to non-linear steepening of the plasma wave.

Evidence for non-linear steepening can be seen in figure 2, which shows W_{max} as a function of plasma density. We find that both the mean and the peak beam energy for both nozzles increase with decreasing density ($W_{max} \propto n_e^{-1}$) down to a certain density threshold, below which there is no self-injection. This threshold is close to the density at which the matched spot size is no longer smaller than the vacuum focal spot size, so that there is no transverse intensity amplification. The mean and peak energies for the 5 mm nozzle and the average beam energy for the 10 mm nozzle above this threshold are predicted by the nonlinear scaling model for a_0 = 3.9, close to our average vacuum laser strength. However the maximum W_{max}, is fitted by a higher $a_0 \approx$ 6.0. This indicates that for ideal guiding, the wakefield amplitude is increased due to the effects of pulse evolution and intensity amplification.

Intensity (a_0) amplification occurs because of pulse compression[18] and photon deceleration[19], as well as self-focusing. Further evidence for this intensity amplification is seen by the multiple lower energy electron bunches observed at long interaction lengths (e.g. fig. 1c,d). Monoenergetic beam production in a self-injecting laser wakefield is dependent on the space-charge field of the injected electrons being strong enough so as to reduce the wake amplitude and stop injection. The bunch is thus localised in space and

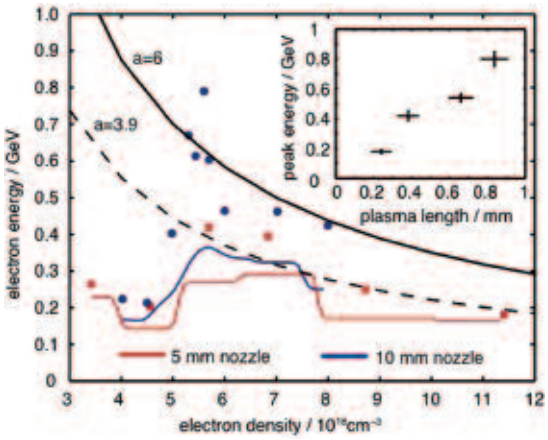

Figure 2. Scaling of peak and mean electron beam energy with plasma density. Peak electron energy is given in red squares and blue circles, for the 5 mm and 10 mm gas jet, respectively. Mean electron energy is given by the red and blue line, for the 5 mm and 10 mm gas jet, respectively. The mean was calculated with a moving kernel of gaussian shape. The laser energy and pulse length were 10.0 (±1.5) J on target and τ = 55 (±5) fs. The best fit lines shown in black are the non-linear wakefield scaling laws[9]. The mean obser ved energy is close to that for $a_0 \approx 3.9$ which is the expected vacuum focused intensity a_0, whilst the best fit for the highest obser ved energies is for $a_0 \approx 6.0$, giving evidence for a_0 amplification under ideal guiding conditions. The inset shows the maximum observed electron energy as a function of plasma length.

consequently, as the electrons are accelerated by almost the same fields, also in phase space. Intensity amplification means that the plasma wave amplitude also continues to rise, allowing further injection. The bunches which break when the wakefield amplitude has increased due to the intensity amplification experience a larger wake amplitude and thus can be accelerated to higher energies. Of course, for this to be possible, the laser pulse must be self-guided over multiple z_R.

Figure 3 depicts multiple views of the laser propagation through the plasma. Side imaging (interferometry - figure 3a) shows a plasma with channel size increasing at an angle similar to that of the $F = 20$ focusing optic used. Figure 3d,e shows the beam profile after transmission through 10 mm of plasma at high intensity. The profiles show a central bright spot comparable in size to the initial beam focus (figure 3b), with an outer halo that is comparable to the laser beam profile when the laser is propagated in vacuum (figure 3c). The expanding plasma cone is produced by the unguided halo, but there is a central guided filament which propagates at sufficiently high intensity to drive a large amplitude plasma wave. By noting that there is typically 30% energy transmission at the end of the interaction, and that half of this transmitted energy in the central spot (of $2w_0 = 22$ μm ~ λ_p), we calculate that there is $P \approx 5$ TW within the guided central filament. This compares favourably with the value of P_c for this threshold density.

Fully relativistic 3D particle in cell simulations were perfomed with parameters matching experimental values. Figure 4 shows the accelerating structure after a distance of 4.8 mm. The laser pulse has been self-guided over this distance and drives a highly non-linear plasma wave. The plasma wave self-injects early in the simulation and there is strong beam loading due to the injected electrons. The acceleration occurs in two phases. The electron bunch at the head of the injected beam is rapidly accelerated to ~500 MeV and then is decelerated as it dephases. As the laser propagates, the rear self-focuses and the head is continually being self-amplifed due to temporal compression. This results in a continual stream of injection, and a large number of electrons is injected into the bubble. Also because of the increasing plasma wave amplitude, the maximum energy which they attain before dephasing is higher[14]. At the time shown in figure 4, the secondary bunch has phase rotated, leading to a narrow energy spread feature in the electron spectrum at 0.8 GeV in good agreement with experimental measurements. The maximum energy gain is due to the combination of beam loading and dephasing in the accelerating structure. The laser is self-guided over the whole range of the gas jet as in the experiment. However at later times, there is little further gain in electron energy due to dephasing, and an electron beam at close to the maximum energy exits the gas jet. The simulations confirm that a high intensity laser beam can be self-guided over sufficient lengths to enable energy gains in excess of gigaelectronvolts.

In conclusion, these studies demonstrate that a guiding structure is not essential for laser wakefield acceleration and that GeV electron beams can be obtained from a simple gas jet target. In addition the

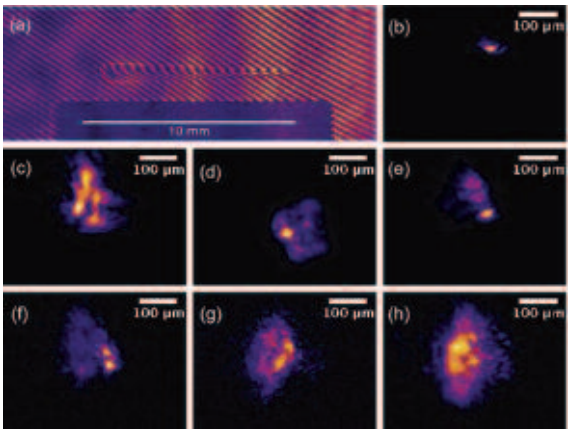

Figure 3. Evidence of laser self guiding over full interaction length. (a) a typical interferogram obtained by transverse probing; a plasma extends the full length of the 10 mm gas jet; (b) to (h) are background subtracted 2D images of the laser mode for various conditions; (b) in vacuum at the position of optimal focus $z = 0$, revealing a typical 22(±6) μm focus; (c) in vacuum at $z = 10$ mm (or $\approx 13\ z_R$), showing a diffracted beam with non-uniform intensity due to non-ideal beam and imaging quality; (d) to (h) at $z = 10$ mm with gas jet activated and laser powers of: (d) 180 TW, (e) 60 TW, (f) 30 TW, (g) 20 TW and (h) 7 TW. (d) and (e) show that a central intense filament can be guided for high laser powers whereas (f) to (h) highlight that self-guiding becomes less effective for decreasing laser powers. All shots taken with τ = 55 fs and $n_e = 5.7\ (\pm 0.2) \times 10^{18}$ cm^{-3}.

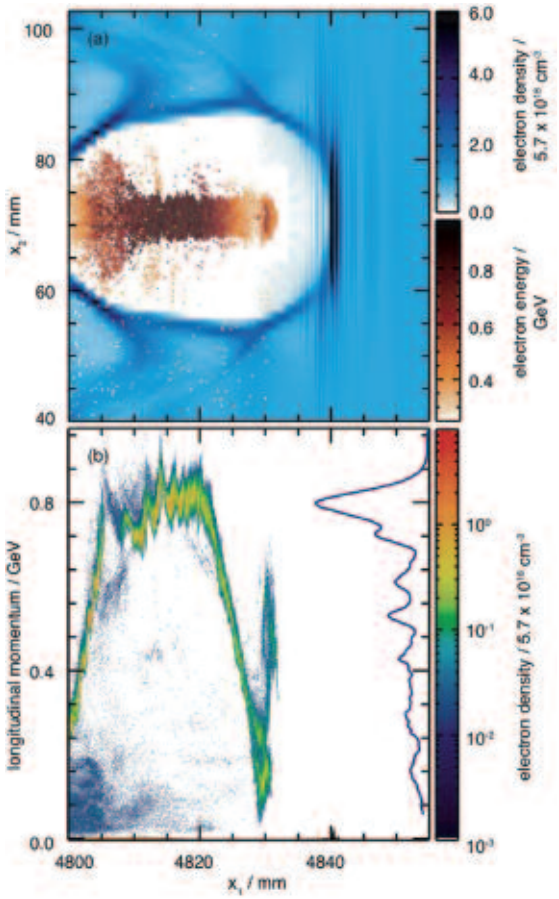

Figure 4. Numerical simulation results for plasma density and electron energy. Simulations obtained with OSIRIS (see simulations section). (a) shows the plasma density (blue) and injected bunch (red). At 4.8 mm into the interaction, strong beam loading is evident. The simulation predicts guiding over the full length of the 10 mm nozzle and amplification in good quantitive agreement with the measurements. (b) represents the longitudinal momentum of electrons across the wakefield. The line on the right axis corresponds to the energy spectrum of the injected electrons (number of electrons in arb. units). The peak electron beam energy maximises at ≈ 0.8 GeV.

open geometry allows access for advanced injection schemes [17,20] and for harnessing plasma waves as radiation sources. This would have a major impact on the uses of GeV electron beams, such as novel radiation sources, making them more compact, economical and abundant, and thus impacting progress all across science and technology.

The authors wish to acknowledge N. Delerue, G. Doucas and D. Urner for their help with the design and operation of the electron spectrometer and N. Bourgeois, T. Ibbotson and S. Hooker for their assistance during the experiment.

Methods

Laser

The experiments were carried out on the Astra Gemini laser system at the Rutherford Appleton Laboratory. Gemini is a dual-beam Ti:sapphire laser with central wavelength λ_0 = 800 nm which operates using chirped pulse amplification. For these studies, a single beam of maximum power of P = 250 TW was used. The temporal shape of the laser pulse is gaussian, with a typical duration of τ = 55 ± 5 fs at full-width half-maximum (FWHM). The laser beam was linearly polarised and focused onto the target with an off-axis parabolic mirror with focal length of f = 3 m. The ratio of f to beam diameter, the F number was F = 20. The laser pulse carried up to 12 J of energy and was focused to a peak intensity of $(1.9 \pm 0.2) \times 10^{19}$ Wcm^{-2}, which gives a corresponding normalised vector potential $a_0 \equiv \frac{eE}{m\omega c} \approx 3.9$, where E is the peak electric field strength of the laser and ω is its frequency. The transverse profile of the laser in vacuum yields a focal spot diameter of $2w_{HWHM}$ = (22.0 ± 6) μm or $w_0 \approx 19$ μm at $1/e^2$ of intensity. The Rayleigh length is thus, $z_R = 2Fw_0 \approx 760$ μm, which was supported by experimental measurements. Typically (31± 2) % of the pulse energy is within the diameter 2 w_{HWHM}.

Gas Jet

The targets were supersonic helium gas jets with varying nozzle diameter of 3, 5, 8 and 10 mm. The laser was focused 1.5 mm above the front edge of the nozzle. The plasma density profile measured by interferometry has a FWHM length of 2.7 ± 0.2 mm, 4.1 ± 0.2 mm, 6.8 ± 0.3 mm and 8.7 ± 0.3 mm for various nozzles and consists of a central plateau, which is constant to within 10%, and linear gradients at the edges.

Electron Spectrometer

The electron spectrometer is based on a dipole electromagnet with circular pole pieces of radius 167 mm. The magnetic field strength was a function of the applied current, with a maximum of 1.15 T. The electron spectrometer disperses the beam onto a phosphor screen (Kodak Lanex Regular) which is imaged onto a CCD camera. A tracking code using the measured magnetic field map relates the measured beam defiection to an electron energy. Error bars are given by the acceptance angle of the electron spectrometer and are $\Delta E/E$ = 6 % at 0.8 GeV for the data shown in figure 1c. The phosphor screen was cross calibrated with an image plate (Fuji BAS MS) for absolute electron charge measurements.

Simulations

Numerical simulations were performed with OSIRIS [21], a fully relativistic, electromagnetic, massively parallel particle-in-cell code [22]. Plasma is simulated by a set of quasi-particles moved under the action of self-consistent electromagnetic fields; first the current density is deposited on a spatial grid, then Maxwell's equations are solved on the same grid, finally the acceleration on each particle is computed by interpolating the field values in the position of the point particle. Results are for a three-dimensional simulation of a linearly polarized, diffraction limited laser pulse with a_0 = 3.9 focused at the entrance of the plasma. The longitudinal profile of the laser electric field is symmetric and given by $10\tau^3 - 15\tau^4 + 6\tau^5$, with $\tau = (t - t_0)/\tau_{FWHM}$, and τ_{FWHM} = 55 fs. The transverse profile of the laser is gaussian with a spot of $2w_{HW\,HM}$ = 22 μm. The plasma density profile increases linearly from zero to $n_e = 5.7 \times 10^{18}$ cm^{-3} in the first 650 μm, is constant for 7317 μm, and falls

linearly to zero in 1180 μm. In the transverse direction, the plasma density falls linearly from the center to 5.1×10^{18} cm^{-3} at the edges of the box. The window is $71 \times 143 \times 143$ μm^3, follows the laser, and has $3500 \times 256 \times 256$ cells. A total of 2.3×10^8 particles with second order shapes were pushed for 5×10^5 iterations (1 week computing time on a 256 node cluster). The resolution in the laser propagation direction z is $k_0\Delta z = 0.16$, and $k_p\Delta x = k_p\Delta y = 0.25$ in the transverse directions.

References

1. I. Blumenfeld, *et al.*, Energy doubling of 42 Gev electrons in a metre-scale plasma wakefield accelerator. *Nature* **445**, 741 (2007).
2. W. P. Leemans, *et al.*, Gev electron beams from a centimetre-scale accelerator. *Nature Phys*. **2**, 696 (2006).
3. T. Tajimaand J. M. Dawson, Laser electron accelerator. *Phys. Rev. Lett*. **43**, 267 (1979).
4. A. Modena, *et al.*, Electron acceleration from the breaking of relativistic plasma-waves. *Nature* **377**, 606–608 (1995).
5. K. Nakajima, *et al.*, Observation of ultrahigh gradient electron acceleration by a self-modulated intense short laser pulse. *Phys. Rev. Lett*. **74**, 4428–4431 (1995).
6. S. P. D. Mangles, *et al.*, Monoenergetic beams of relativistic electrons from intense laser-plasma interactions. *Nature* **431**, 535 (2004).
7. C. G. R. Geddes, *et al.*, High-quality electron beams from a laser wakefield accelerator using plasma-channel guiding. *Nature* **431**, 538 (2004).
8. J. Faure, *et al.*, A laser-plasma accelerator producing monoenergetic electron beams. *Nature* **431**, 541 (2004).
9. W. Lu, *et al.*, Generating multi-GeV electron bunches using single stage laser wakefield acceleration in a 3D nonlinear regime. *Phy. Rev. Sp. Top. Acc. Beams* **10** (2007).
10. A. G. R. Thomas, *et al.*, Effect of laser-focusing conditions on propagation and monoenergetic electron production in laser-wakefield accelerators. *Phys. Rev. Lett*. **98**, 095004 (2007).
11. G.-Z. Sun, E. Ott, Y. C. Lee and P. Guzdar, Self-focusing of short intense pulses in plasmas. *Phys. Fluids* **30**, 526 (1987).
12. F. S. Tsung, *et al.*, Near-gev-energy laser-wakefield acceleration of self-injected electrons in a centimeter-scale plasma channel. *Phys. Rev. Lett*. **93**, 185002 (2004).
13. T. P. Rowlands-Rees, *et al.*, Laser-driven acceleration of electrons in a partially ionized plasma channel. *Phys. Rev. Lett*. **100**, 105005 (2008).
14. W. Lu, C. Huang, M. Zhou, W. B. Mori, and T. Katsouleas. Nonlinear theory for relativistic plasma wakefields in the blowout regime. *Phys. Rev. Lett*. **96**, 165002 (2006).
15. A. Pukhov and J. Meyer-ter Vehn. Laser wakefield acceleration: the highly non-linear broken-wave regime. *Appl. Phys. B: Lasers Opt*. **74**, 355–361 (2002).
16. C.-T. Hsieh, *et al.*, Tomography of injection and acceleration of monoenergetic electrons in a laser-wakefield accelerator. *Phys. Rev. Lett*. **96**, 095001 (2006).
17. J. Faure, *et al.*, Controlled injection and acceleration of electrons in plasma wakefields by colliding laser pulses. *Nature* **444**, 737–739 (2006).
18. J. Faure, *et al.*, Observation of laser-pulse shortening in nonlinear plasma waves. *Phys. Rev. Lett*. **95**, 205003 (2005).
19. C. D. Murphy, *et al.*, Evidence of photon acceleration by laser wake fields. *Phys. Plasmas* **13**, 033108. (2006).
20. D. Umstadter, J. K. Kim and E. Dodd. Laser injection of ultrashort electron pulses into wakefield plasma waves. *Physical Review Letters* **76**, 2073–2076 (1996).
21. R. A. Fonseca. *Lecture Notes in Computer Science 2329*, vol. III-342 (Springer, Heidelberg, 2002).
22. J. M. Dawson. Particle simulation of plasmas. *Review of Modern Physics* **55**, 403 (1983).
23. S. P. D. Mangles, *et al.*, Laser-wakefield acceleration of monoenergetic electron beams in the first plasma-wave period. *Phys. Rev. Lett*. **96**, 215001 (2006).